

Published in final edited form as:

*J Med Chem.* 2008 April 24; 51(8): 2447–2456. doi:10.1021/jm701384x.

## Polyaminohydroxamic Acids and Polyaminobenzamides as Isoform Selective Histone Deacetylase Inhibitors§

Sheeba Varghese<sup>†</sup>, Thulani Senanayake<sup>†</sup>, Tracey Murray-Stewart<sup>‡</sup>, Kim Doering<sup>‡</sup>, Alison Fraser<sup>‡</sup>, Robert A. Casero Jr.<sup>‡</sup>, and Patrick M. Wooster<sup>†,\*</sup>

<sup>†</sup>Department of Pharmaceutical Sciences, Wayne State University, 259 Mack Avenue, Detroit, Michigan 48202

<sup>‡</sup>Sidney Kimmel Comprehensive Cancer Center, Johns Hopkins University, Baltimore, Maryland 21231

### Abstract

A series of polyaminohydroxamic acids (PAHAs) and polyaminobenzamides (PABAs) were synthesized and evaluated as isoform-selective histone deacetylase (HDAC) inhibitors. These analogues contain a polyamine chain to increase affinity for chromatin and facilitate cellular import. Seven PAHAs inhibited HDAC >50% (1  $\mu$ M), and two PABAs inhibited HDAC >50% (5  $\mu$ M). Compound **17** increased acetylated  $\alpha$ -tubulin in HCT116 colon tumor cells 253-fold but only modestly increased p21<sup>waf1</sup> and acetylated histones 3 and 4, suggesting that **17** selectively inhibits HDAC 6. PABA **22** alone minimally increased p21<sup>waf1</sup> and acetylated histones 3 and 4 but caused dose-dependent increases in p21<sup>waf1</sup> in combination with 0.1  $\mu$ M 5-azadeoxycytidine. Finally, **22** appeared to be a substrate for the polyamine transport system. None of these compounds were cytotoxic at 100  $\mu$ M. PAHAs and PABAs exhibit strikingly different cellular effects from SAHA and have the potential for use in combination antitumor therapies with reduced toxicity.

### Introduction

The dynamic status of acetylation on specific histone lysine residues, mediated by histone acetyltransferases (HATs) and histone deacetylases (HDACs),<sup>a</sup> plays a critical role in the regulation of gene expression.<sup>1,2</sup> In some tumor cell types, hypoacetylation of histones caused by aberrant HDAC activity results in the underexpression of growth regulatory factors such as the cyclin dependent kinase inhibitor p21<sup>waf1</sup> (also known as CDKN1A and CIP1) and thus contributes to the development of cancer.<sup>1,2</sup> Histone hyperacetylation caused by HDAC inhibitors such as trichostatin A (TSA, **1**), *N*-(2-aminophenyl)-4-[*N*-(pyridin-3-ylmethoxycarbonyl)aminomethyl]benzamide **2** (MS-275),<sup>3</sup> and SAHA (**3**) (Figure 1) can cause growth arrest in a wide range of transformed cells and can inhibit the growth of human tumor xenografts.<sup>1,2,4,5</sup> Both **2** and **3** are effective in the clinic, especially when used in combination with DNA methyltransferase inhibitors such as 5-aza-2'-deoxycytidine (5-azadC).<sup>6</sup> Although they are effective both in vitro and in vivo, HDAC inhibitors typified by **1–3** inhibit multiple isoforms of HDAC and produce side effects through activity in noncancerous cells. Thus, it is desirable to identify potent HDAC inhibitors that restore the

§This manuscript is dedicated to Professor James K. Coward on the occasion of his retirement.

© 2008 American Chemical Society

\*To whom correspondence should be addressed. Phone: 313-577-1523, Fax: 313-577-2033. pwoster@wayne.edu.

<sup>a</sup>Abbreviations: HAT, histone acetyltransferase; HDAC, histone deacetylase, SAHA, suberoylanilide hydroxamic acid; PAHA, polyaminohydroxamic acid; PABA, polyaminobenzamide; 5-aza-dC, 5-aza-2'-deoxycytidine; AcTubulin, acetylated R-tubulin; MTS, 3-(4,5-dimethylthiazol-2-yl)-5-(3-carboxymethoxyphenyl)-2-(4-sulfophenyl)-2H-tetrazolium, inner salt.

expression of normal tumor suppressor genes without producing significant dose-limiting toxicity.<sup>6</sup> Current structure-activity studies involving analogues of **1–3** have focused largely on modifications to the aromatic ring moiety and the aliphatic linker region present in these molecules.<sup>5,7</sup> We recently reported a series of polyaminohydroxamic acid (PAHA) derivatives that incorporate structural features of the polyamines spermidine and spermine (**4** and **5**, respectively, Figure 1) and the linker and hydroxamic acid moieties found in **1** and **3**.<sup>8</sup> This strategy is based on the observation that polyamine analogues have high affinities for DNA<sup>9–12</sup> and enter cells using the cellular polyamine transport system.<sup>9,13</sup> Thus, PAHAs could be selectively directed to DNA and the associated histones. It has been shown that HDAC isoforms have a high degree of sequence homology in the binding pocket but differ in primary sequence at residues in the rim region outside the lysine residue binding site.<sup>4</sup> Thus, it may be possible to produce isoform specific inhibitors for individual HDACs by altering the polyamine chain composition and its associated terminal alkyl group, since these portions of the molecule would be expected to interact with the rim region. Using these design criteria, we successfully identified three lead compounds from a library consisting of only 16 analogues.<sup>8</sup> We now report 15 additional analogues in the PAHA series (compounds **6–20**) and have extended our studies to include polyaminobenzamides (PABAs) **21–23**, which incorporate the benzamide moiety of **2** and also possess HDAC inhibitory activity in vitro.

## Chemistry

PAHA analogues **6–20** (Table 1) were synthesized using routes that were previously described.<sup>8</sup> The synthetic routes to PABA analogues **21–23** are shown in Schemes 1 and 2. Our initial strategy involved *N*-Boc protection<sup>14</sup> of 4-(amino)methylbenzoic acid **24**, followed by coupling with *o*-nitroaniline (EDCI, HOBT, TEA) to form **25**.<sup>15,16</sup> Compound **25** was then appended to the protected carboxylate **26**<sup>8</sup> as previously described<sup>8</sup> followed by reduction of the nitro group (SnCl<sub>2</sub>)<sup>3,16</sup> and deprotection (30% HBr in AcOH)<sup>8</sup> to afford target benzamide **21**. Although the EDCI coupling to form **25** proceeded in 65% yield, the reaction resulted in multiple side products that complicated purification. In addition, in our hands the reduction of the nitro group produced an unacceptable yield (32%). We thus adopted the synthetic strategy outlined in Scheme 2. *o*-Aminoaniline **27** was mono-*N*-Boc protected<sup>14,16</sup> to form **28** in 80% yield. Commercial 4-(methoxycarbonyl)benzylamine **29** was then coupled to the previously described intermediates **30a** and **30b**<sup>8,17</sup> to afford compounds **31a** and **31b** in 95.3% and 92.4% yield, respectively. Hydrolysis of the ester (1.0 N LiOH) yielded the corresponding carboxylates **32a** and **32b**, which were coupled to **28**<sup>8,17</sup> to form **33a** and **33b**. Removal of the mesityl protecting groups (30% HBr in AcOH)<sup>18,19</sup> then afforded the desired benzamides **22** and **23** (average of 74% yield from **31**).

## Biological Evaluation

PAHAs **6–20** were evaluated for their ability to inhibit isolated HDAC activity at 1  $\mu$ M in the Fluor de Lys assay system (Biomol International LP, Plymouth Meeting, PA), employing 1.0  $\mu$ M TSA (**1**) as a positive control.<sup>8</sup> The results of these studies are summarized in Table 1. PAHAs **6**, **8**, **9**, **13**, **17**, **18**, and **20** all produced greater than 50% inhibition, with compound **18** producing the greatest inhibition (88.7%). Under the same conditions, TSA produced 100% inhibition of the enzyme. PABA analogues **21–23** were similarly evaluated at concentrations of 5.0  $\mu$ M, using 5.0  $\mu$ M **2** as a positive control. Compounds **21–23** produced 37.4%, 51.2%, and 66.7% inhibition, respectively (Figure 2), compared to 51.6% inhibition by **2** at the same concentration. Dose-response experiments (not shown) revealed that **22** and **23** possess IC<sub>50</sub> values of 4.9 and 3.8  $\mu$ M, respectively, which compares favorably to the IC<sub>50</sub> value of 4.8  $\mu$ M reported for **2**.<sup>3</sup>

Compounds **9–18**, **20**, and **22** were next evaluated for their ability to promote in vitro re-expression of the cyclin-dependent kinase inhibitor p21<sup>waf1</sup>, in cultured HCT116 human colon carcinoma cells, as shown in Table 2. These analogues were also assayed for their ability to promote increased acetylated histones H3 and H4 (AcH3, AcH4) and acetylated R-tubulin (AcTubulin). Following treatment for 24 h, the effects of **9**, **10**, **12**, **14**, **18–20** were unremarkable. However, as summarized in Figure 3, PAHAs **11**, **13**, **15–17** all promoted a >50-fold increase in acetylated R-tubulin in the HCT116 cell line (Figure 3A). In the case of **17**, AcTubulin levels increased more than 253-fold. By contrast, PABA **22** had no significant effect on the acetylation status of this protein. Each compound also produced significant effects on p21<sup>waf1</sup> re-expression, and all were more effective than SAHA (**3**) in this regard (Figure 3B). These analogues also produced slight to moderate increases in the levels of AcH3 and AcH4. Under these conditions, **3** caused no increase in p21<sup>waf1</sup>, a modest increase (13.2-fold) in AcTubulin, and 30.7- and 106-fold increases in AcH3 and AcH4, respectively.

Benzamide **22**, which exhibited an IC<sub>50</sub> of 4.9 μM against HDAC in the Fluor de Lys assay system, was evaluated in combination with 0.1 μM of the DNA methyltransferase inhibitor 5-aza-2'-deoxycytidine (5-aza-dC) for additive or synergistic effects with respect to re-expression of p21<sup>waf1</sup>, as well as p16, a tumor suppressor gene important for cell cycle regulation (Figure 4). In the HCT116 cell line, no additive effects were observed for the re-expression of p16, whose levels appeared to decrease slightly in the presence of either **22** alone or **22** plus pretreatment with 0.1 μM 5-aza-dC. By contrast, dose-dependent additive effects were observed in the re-expression of p21<sup>waf1</sup> when treatment with increasing concentrations of **22** was preceded by treatment with 0.1 μM 5-aza-dC.

A <sup>14</sup>C-spermidine uptake competition assay<sup>20,21</sup> was conducted to determine whether PAHAs or PABAs are substrates for the polyamine transport system in the ML-1 acute myelogenous leukemia cell line. In the case of all PAHA analogues tested, no competition for the uptake of <sup>14</sup>C-spermidine was observed, suggesting that PAHAs are not taken up into cells by the polyamine transporter. At physiological pH, the hydroxamic acid moiety (pK<sub>a</sub> ≈ 8.8) is less than 5% ionized. However, in unrelated experiments, we have observed that polyamine analogues with terminal, oxygen-containing substituents that can ionize at physiological pH are poor substrates for the polyamine transport system (unpublished observations). This is consistent with the hypothesis that, rather than being a membrane-bound proteinaceous transporter, the mammalian polyamine transport system may operate by attracting positively charged substrates, followed by endocytosis,<sup>20</sup> in which case negatively charged substrates would be less likely to bind to the membrane receptor. However, the lack of transport of these molecules does not formally preclude the two-step pathway proposed by Poulin and colleagues.<sup>21</sup> By contrast, benzamide **21** produced a noncompetitive inhibition of <sup>14</sup>C-spermidine uptake (K<sub>i</sub> = 7.7 μM, Figure 5), suggesting that it is readily accumulated through the polyamine transporter.

The cytotoxicity of compounds **6–23** was determined in the HCT116 colon carcinoma cell line using a standard 3-(4,5-dimethylthiazol-2-yl)-5-(3-carboxymethoxyphenyl)-2-(4-sulfophenyl)-2H-tetrazolium (MTS) reduction assay procedure after 96 h of treatment. The results of these studies are summarized in Table 3. The traditional HDAC inhibitor SAHA (**3**) was found to have an IC<sub>50</sub> value of 1.8 μM in the HCT116 cell line. By contrast, IC<sub>50</sub> values for compounds **6–19** and **21–23** were all found to be >100 μM under the same conditions. Compound **20**, which inhibited HDAC activity by 58.6% at a concentration of 1.0 μM, was initially found to have IC<sub>50</sub> values of 38.6 and 47.2 μM against the HCT116 line. However, in the presence of 1.0 mM aminoguanidine, a diamine oxidase inhibitor, this effect was completely abolished. Compound **20** possesses a terminal primary amine moiety,

and thus, the observed cytotoxicity is likely the result of the production of toxic metabolites by serum amine oxidases.

## Discussion

Clinical studies indicate that HDAC inhibitors such as **2** are effective therapies for human cancer,<sup>22</sup> but dose-limiting toxicity remains a problem.<sup>6,23</sup> HDAC inhibitors partially restore normal cell cycle and apoptotic functions in human tumor cells. In vitro models have demonstrated that synergistic re-expression of genes silenced by promoter hypermethylation can be achieved by the sequential application of deoxynucleotide methyltransferase inhibitors and HDAC inhibitors.<sup>24</sup> Phase I trials sequencing 2'-deoxy-5-azacytidine (5-aza-dC) with HDAC inhibitors in patients with acute myelocytic leukemia demonstrate a correlation between chromatin remodeling and clinical efficacy, and robust clinical responses have developed at rates higher than treatment with either demethylating agents or HDAC inhibitors alone.<sup>24,25</sup> However, step-down dosing of the HDAC inhibitors in these combinations is often required to minimize toxicity. Consequently, effective HDAC inhibitors having minimal inherent toxicity on their own may provide excellent candidates for combination with agents like 5-aza-dC. Thus, compounds such as those described in this manuscript could be used as part of a combination therapy approach with a lower overall incidence of adverse side effects.

Not surprisingly, in the PAHA series, the length of the linker chain adjacent to the hydroxamic acid metal binding group appears to have a dramatic effect on HDAC inhibitory activity (Table 1). For example, HDAC inhibition increases for compounds **7–9** as the length of the chain increases from five to eight carbons. Compound **18**, the most effective inhibitor in this series, has a seven-carbon linker chain. However, the inhibitory activity of **13** cannot be explained on the basis of linker length, suggesting that other factors can contribute to the activity of PAHAs. It is noteworthy that the most active inhibitors, compounds **9**, **13**, and **18**, are significantly more active than compounds **19** and **20**, which contain a traditional “cap” group that is thought to bind to a surface region in the HDAC active site.<sup>1,2,4</sup> Linker length also appears to play a role in the activity of PABAs **21–23** (Figure 2), although more analogues will need to be examined to make any structure-function correlations.

When the cellular effects of PAHAs **6–20** and PABA **22** are examined, distinct differences from the effects of the traditional HDAC inhibitor SAHA are observed. Since the linker and metal binding moieties of compounds **6–20** are identical to or close homologues of SAHA, these differences in specificity of cellular effects are most likely due to the polyamine portion of the molecules. The compounds shown in Figure 3 produce much greater effects on the levels of AcTubulin than SAHA, **3**. These compounds possess either a four-carbon (as in **11**, **13**, and **15**), five-carbon (as in **17**), or six-carbon (as in **16**) linker chain, which is comparable to the six-carbon linker chain of **3**, supporting the contention that the observed effect on AcTubulin is mediated through the polyamine portion of the molecule. Compound **17**, with a five-carbon linker, produced the greatest increase in the expression of AcTubulin (>253-fold). It is noteworthy that none of the analogues that increased the levels of AcTubulin have the so-called “cap” group that is present in linker chain of **3** and that is thought to bind to the surface binding area of the HDAC active site. The ability of PAHAs to increase the levels of AcTubulin does not correlate with their ability to inhibit HDAC in the commercial assay containing all of the HDAC isoforms. However, such a correlation may exist with HDAC 6 activity alone, or the increase in AcTubulin may be due to interaction of these PAHAs with another site. Nonetheless, the data suggest that compounds such as **17** selectively inhibit HDAC 6. As was mentioned above, compound **17** produced 51.5% inhibition of HDAC isoforms in a HeLa cell lysate HDAC at 1 μM. In a preliminary study involving recombinant HDAC isoforms 3 and 6, it was determined that **17** produced

99.1% and 99.7% inhibition of HDACs 3 and 6, respectively. This inhibition profile is consistent with the high degree of induction of AcTubulin re-expression by **17**. The inhibition of recombinant HDAC 3 and 6 is now being determined for all of the analogues reported in this manuscript, and the results of these experiments are forthcoming.

As shown in Table 2 and Figure 3, 10.0  $\mu\text{M}$  PABA **22** caused a 2.55-fold increase in the expression of p21<sup>waf1</sup> in the HCT116 cell line. This compound is structurally similar to **17** except that it has a six-carbon (rather than five-carbon) linker and has a benzamide in place of the hydroxamic acid metal binding moiety. However, unlike **17**, PABA **22** did not increase the expression of AcH3 and AcH4 and only increased AcTubulin expression by 2-fold. Compound **22** was also evaluated as an inhibitor of recombinant HDACs 3 and 6, and produced a 1.3% and 11.7% inhibition of these isoforms, respectively. This inhibition profile is consistent with the absence of induction of AcTubulin re-expression by **22**. The data shown in Figure 4 demonstrate that **22** reduced the expression of p16 and had only a moderate effect on p21<sup>waf1</sup> levels (1.63-fold at 25  $\mu\text{M}$ ). When **22** was combined with the known p16/p21<sup>waf1</sup> inducer 5-azadC, no re-expression of p16 was observed. However, the combination of **22** and 5-aza-dC produced an additive, dose dependent increase in p21<sup>waf1</sup> levels.

The polyamine transport system, which is known to import the natural polyamines and a variety of their analogues, is up-regulated in most tumor cell types.<sup>26</sup> As discussed above, none of the PAHA analogues tested were taken up by the polyamine transport system. However, PABA **21** was shown to be an effective noncompetitive inhibitor of the uptake of <sup>14</sup>C-spermidine, suggesting that it is a substrate for the polyamine transport system. Because the polyamine transport system is highly active in tumor cells, PABAs related to **21** have the potential to be preferentially imported into tumor cells in high concentrations.

As shown in Table 3, PAHAs **6–20** and PABAs **21–23** exhibited IC<sub>50</sub> values greater than 100  $\mu\text{M}$  in the HCT116 colon carcinoma cell line. By contrast, **3** is significantly more cytotoxic, with an IC<sub>50</sub> value of 1.8  $\mu\text{M}$  in the HCT116 line. As was pointed out above, there may be advantages to administration of an HDAC inhibitor that effectively promotes the re-expression of aberrantly silenced genes with minimal inherent toxicity. In tumor therapy, such agents could be used in place of HDAC inhibitors with dose limiting side effects, in order to decrease the overall toxicity to normal tissue during combination chemotherapy. In addition, such agents may prove useful in disease states such as diabetes, where HDACs play a role, but cytotoxicity is not an acceptable end point. The synthesis of additional analogues in the PAHA and PABA series is an ongoing concern in our laboratories. In addition, the analogues described herein are now being evaluated as inhibitors of individually expressed HDAC isoforms, which are now available commercially. The results of these studies, as well as in vivo efficacy studies of **17** and **22** in a mouse xenograft model, will be reported in a future manuscript.

## Experimental Section

All reagents and dry solvents were purchased from Aldrich Chemical Co. (Milwaukee, WI), Sigma Chemical Co. (St. Louis, MO), or Acros Chemical (Chicago, IL) and were used without further purification except as noted below. Pyridine was dried by passing it through an aluminum oxide column and then stored over KOH. Triethylamine was distilled from potassium hydroxide and stored in a nitrogen atmosphere. Methanol was distilled from magnesium and iodine under a nitrogen atmosphere and stored over molecular sieves. Methylene chloride was distilled from phosphorus pentoxide, and chloroform was distilled from calcium sulfate. Tetrahydrofuran was purified by distillation from sodium and benzophenone. Dimethylformamide was dried by distillation from anhydrous calcium

sulfate and was stored under nitrogen. Preparative scale chromatographic procedures were carried out using E. Merck silica gel 60, 230–440 mesh. Thin layer chromatography was conducted on Merck precoated silica gel 60 F-254. Ion exchange chromatography was conducted on Dowex 1X8-200 anion exchange resin. Compounds **26**, **30a**, and **30b** (Schemes 1 and 2) were synthesized as previously described.<sup>8</sup>

All <sup>1</sup>H and <sup>13</sup>C NMR spectra were recorded on a Varian Mercury 400 MHz spectrometer, and all chemical shifts are reported as δ values referenced to TMS or DSS. Infrared spectra were recorded on a Nicolet 5DXB FT-IR spectrophotometer and are referenced to polystyrene. In all cases, <sup>1</sup>H NMR, <sup>13</sup>C NMR, and IR spectra were consistent with assigned structures. Microanalyses were performed by Galbraith Laboratories, Knoxville, TN, and were within 0.4% of calculated values.

Compounds **6–20** were produced using a synthetic scheme that was previously described.<sup>7</sup> Spectral data for each of these analogues are given below.

**20-{N-[(2,2-Diphenyl)propyl]amino}-8-oxo-9,13,17-triazaeicosanohydroxamic Acid Trihydrobromide (6)**

<sup>1</sup>H NMR (CDCl<sub>3</sub>) δ 1.37 (m, 4H), 1.40 (m, 4H), 1.71 (m, 2H), 1.88 (m, 4H), 1.97 (t, *J* = 7.2 Hz, 2H), 2.07 (t, *J* = 7.2 Hz, 2H), 2.30 (q, *J* = 7.6 Hz, 2H), 2.85 (m, 12H), 3.10 (t, *J* = 6.8 Hz, 2H), 3.93 (t, *J* = 8 Hz, 1H), 7.11 (m, 2H), 7.21 (m, 8H). Anal. (C<sub>32</sub>H<sub>54</sub>Br<sub>3</sub>N<sub>5</sub>O<sub>3</sub>) C, H, N.

**16-{N-[(2,2-Diphenyl)propyl]amino}-7-oxo-8,12-diazahexadecanohydroxamic Acid Dihydrobromide (7)**

<sup>1</sup>H NMR (CDCl<sub>3</sub>) δ 1.10 (m, 2H), 1.40 (m, 2H), 1.69 (m, 4H), 1.71 (m, 2H), 1.97 (t, *J* = 6.8 Hz, 2H), 2.06 (t, *J* = 7.2 Hz, 2H), 2.31 (m, 2H), 2.84 (m, 8H), 3.09 (t, *J* = 6.4 Hz, 2H), 3.94 (t, *J* = 7.6 Hz, 1H), 7.11 (m, 2H), 7.21 (m, 8H). <sup>13</sup>C NMR (400 MHz CDCl<sub>3</sub>) 13.38, 20.66, 22.79, 22.89, 24.63, 25.02, 25.78, 27.55, 30.88, 35.57, 36.00, 45.19, 46.47, 46.79, 46.96, 48.11, 61.85, 127.15, 127.64, 129.20, 143.68, 174.84, 177.58. IR (cm<sup>-1</sup>): 3376.6, 2929.7, 2780.5, 1634.5, 1557.5, 1452.4. Anal. (C<sub>29</sub>H<sub>46</sub>Br<sub>2</sub>N<sub>4</sub>O<sub>3</sub>) C, H, N.

**18-{N-[(2,2-Diphenyl)propyl]amino}-9-oxo-10,14-diazaoctadecanohydroxamic Acid Dihydrobromide (8)**

<sup>1</sup>H NMR (CDCl<sub>3</sub>) δ 1.11 (m, 6H), 1.38 (m, 4H), 1.54 (m, 4H), 1.70 (m, 2H), 1.96 (t, *J* = 7.6 Hz, 2H), 2.06 (t, *J* = 7.2 Hz, 2H), 2.32 (m, 2H), 2.84 (m, 8H), 3.10 (t, *J* = 6.8 Hz, 2H), 3.98 (t, *J* = 7.6 Hz, 1H), 7.12 (m, 2H), 7.22 (m, 8H). <sup>13</sup>C NMR (CDCl<sub>3</sub>) δ 13.38, 20.65, 22.78, 22.88, 24.91, 25.33, 25.77, 27.93, 27.99, 30.88, 32.46, 35.77, 35.96, 61.85, 127.15, 127.63, 129.20, 143.68, 174.85, 177.93. IR (cm<sup>-1</sup>) 3420.8, 2936.6, 2845.4, 2793.5, 1637.5, 1554.5, 1450.8. Anal. (C<sub>31</sub>H<sub>50</sub>-Br<sub>2</sub>N<sub>4</sub>O<sub>3</sub>) C, H, N.

**19-N-[(2,2-Diphenyl)propyl]amino-10-oxo-11,15-diazanonadecanohydroxamic Acid Dihydrobromide (9)**

<sup>1</sup>H NMR (CDCl<sub>3</sub>) δ 1.08 (m, 8H), 1.39 (m, 4H), 1.54 (m, 4H), 1.70 (m, 2H), 1.96 (t, *J* = 7.2 Hz, 2H), 2.06 (t, *J* = 7.2 Hz, 2H), 2.31 (q, *J* = 8.0 Hz, 2H), 2.81 (m, 8H), 3.10 (t, *J* = 6.8 Hz, 1H), 7.11 (m, 2H), 7.14–7.24 (m, 8H). <sup>13</sup>C NMR (CDCl<sub>3</sub>) δ 13.38, 20.65, 22.79, 22.88, 24.96, 25.39, 25.77, 27.99, 28.19, 30.87, 32.42, 35.80, 35.96, 38.75, 45.14, 61.85, 71.23, 109.99, 127.15, 127.63, 129.20, 130.12, 143.67, 166.48, 173.72, 174.86, 178.00. Anal. (C<sub>32</sub>H<sub>52</sub>Br<sub>2</sub>N<sub>4</sub>O<sub>3</sub>) C, H, N.

**17-N-[4-[(*N,N*-Dimethylamino)benzyl]amino]-8-oxo-9,13-diazaheptadecanohydroxamic Acid Dihydrobromide (10)**

$^1\text{H}$  NMR ( $\text{CDCl}_3$ )  $\delta$  1.12 (m, 4H), 1.40 (m, 4H), 1.60 (m, 4H), 1.72 (m, 2H), 1.98 (t,  $J = 7.2$  Hz, 2H), 2.08 (t,  $J = 6.8$  Hz, 2H), 2.89 (m, 8H), 3.11 (s, 6H), 3.18 (m, 2H), 7.36 (d,  $J = 8.4$  Hz, 2H), 7.43 (d,  $J = 8.4$  Hz, 2H).  $^{13}\text{C}$  NMR ( $\text{CDCl}_3$ )  $\delta$  13.38, 20.67, 22.83, 22.95, 24.05, 24.88, 25.23, 25.52, 25.77, 27.76, 27.91, 28.09, 31.32, 35.72, 36.01, 61.85, 115.48, 117.49, 120.96, 121.74, 130.02, 131.00, 132.62, 138.98, 141.18, 141.88, 168.77, 177.83. Anal. ( $\text{C}_{25}\text{H}_{47}\text{-Br}_2\text{N}_5\text{O}_3$ ) C, H, N.

**15-N-[4-(Isopropyl)benzyl]amino-6-oxo-7,11-diazapentadecanohydroxamic Acid Dihydrobromide (11)**

$^1\text{H}$  NMR ( $\text{CDCl}_3$ )  $\delta$  1.08 (d,  $J = 7.2$  Hz, 6H), 1.43 (m, 4H), 1.60 (m, 4H), 1.72 (m, 2H), 2.02 (m, 2H), 2.11 (m, 2H), 2.89 (m, 6H), 3.12 (m, 2H), 4.05 (s, 2H), 7.26 (s, 4H). IR ( $\text{cm}^{-1}$ ): 3397.7, 2936.2, 2787.0, 1637.0, 1612.9, 1548.1, 1424.8. Anal. ( $\text{C}_{24}\text{H}_{46}\text{Br}_2\text{N}_4\text{O}_3$ ) C, H, N.

**17-N-[4-(Isopropyl)benzyl]amino-8-oxo-9,13-diazaheptadecanohydroxamic Acid Dihydrobromide (12)**

$^1\text{H}$  NMR ( $\text{D}_2\text{O}$ )  $\delta$  1.08 (d,  $J = 7.2$  Hz, 6H), 1.14 (m, 4H), 1.24 (m, 4H), 1.61 (m, 4H), 1.75 (m, 2H), 2.01 (t, 2H), 2.12 (t, 2H), 2.89 (m, 6H), 3.12 (t, 2H), 4.12 (s, 2H), 7.27 (s, 4H). IR ( $\text{cm}^{-1}$ ): 3539.4, 3468.1, 3402.4, 2941.3, 2787.0, 1634.5, 1612.9, 1483.2, 1431.3. Anal. ( $\text{C}_{25}\text{H}_{46}\text{-Br}_2\text{N}_4\text{O}_3$ ) C, H, N.

**15-N-[2-(Phenyl)benzyl]amino-6-oxo-7,11-diazapentadecanohydroxamic Acid Dihydrobromide (13)**

$^1\text{H}$  NMR ( $\text{CDCl}_3$ )  $\delta$  1.14 (m, 4H), 1.33 (m, 2H), 1.41 (m, 6H), 1.71 (m, 2H), 1.99 (t,  $J = 7.2$  Hz, 2H), 2.09 (t,  $J = 7.6$  Hz, 2H), 2.65 (t,  $J = 7.6$  Hz, 2H), 2.76 (t,  $J = 8$  Hz, 2H), 3.12 (t,  $J = 6.8$  Hz, 2H), 4.17 (s, 2H), 7.28 (m, 3H), 7.36–7.45 (m, 6H). IR ( $\text{cm}^{-1}$ ): 3539.4, 3461.6, 3414.9, 2953.9, 2851.8, 1636.3, 1612.9, 1561.0, 1457.3, 1431.3. Anal. ( $\text{C}_{26}\text{H}_{40}\text{Br}_2\text{N}_4\text{O}_3$ ) C, H, N.

**17-N-[2-(Phenyl)benzyl]amino-8-oxo-9,13-diazaheptadecanohydroxamic Acid Dihydrobromide (14)**

$^1\text{H}$  NMR ( $\text{CDCl}_3$ )  $\delta$  1.31 (m, 2H), 1.41 (m, 6H), 1.70 (m, 2H), 2.01 (m, 2H), 2.11 (m, 2H), 2.64 (m, 2H), 2.75 (m, 2H), 2.83 (m, 2H), 3.12 (m, 2H), 4.16 (s, 2H), 7.21 (m, 1H), 7.42 (m, 9H). IR ( $\text{cm}^{-1}$ ): 3552.4, 3474.5, 3414.0, 3228.1, 2955.6, 2806.4, 1637.9, 1612.9, 1554.5, 1450.8, 1431.3. Anal. ( $\text{C}_{28}\text{H}_{44}\text{Br}_2\text{N}_4\text{O}_3$ ) C, H, N.

**15-N-[2-[(Phenyl)thio]ethyl]amino-6-oxo-7,11-diazapentadecanohydroxamic Acid Dihydrobromide (15)**

$^1\text{H}$  NMR ( $\text{CDCl}_3$ )  $\delta$  1.42 (m, 4H), 1.58 (m, 4H), 1.73 (m, 2H), 2.03 (m, 2H), 2.11 (m, 2H), 2.91 (m, 6H), 3.12 (m, 6H), 7.2–7.3 (m, 4H).  $^{13}\text{C}$  NMR ( $\text{CDCl}_3$ )  $\delta$  22.73, 22.90, 24.52, 24.78, 25.78, 29.39, 35.44, 36.06, 45.22, 47.01, 127.79, 129.73, 130.13, 130.63, 132.78, 177.18. Anal. ( $\text{C}_{21}\text{H}_{38}\text{Br}_2\text{N}_4\text{O}_3\text{S}$ ) C, H, N.

**17-N-[2-[(Phenyl)thio]ethyl]amino-8-oxo-9,13-diazaheptadecanohydroxamic Acid Dihydrobromide (16)**

$^1\text{H}$  NMR ( $\text{CDCl}_3$ )  $\delta$  1.15 (m, 4H), 1.41 (m, 4H), 1.57 (m, 4H), 1.72 (m, 2H), 1.99 (t,  $J = 7.6$  Hz, 2H), 2.08 (t,  $J = 7.2$  Hz, 2H), 2.87 (m, 6H), 3.11 (m, 6H), 7.13–7.36 (m, 4H).  $^{13}\text{C}$  NMR ( $\text{CDCl}_3$ )  $\delta$  24.88, 25.24, 25.78, 27.77, 27.93, 29.39, 35.72, 36.01, 45.20, 46.17, 46.99, 127.80, 129.71, 129.74, 130.60, 130.63. Anal. ( $\text{C}_{23}\text{H}_{42}\text{Br}_2\text{N}_4\text{O}_3\text{S}$ ) C, H, N.

**16-*N*-[4-(*tert*-Butyl)benzyl]amino-7-oxo-8,12-diazahexadecanohydroxamic Acid Dihydrobromide (17)**

$^1\text{H}$  NMR ( $\text{CDCl}_3$ )  $\delta$  1.14 (s, 9H), 1.42 (m, 4H), 1.59 (m, 4H), 1.70 (m, 2H), 1.99 (m, 2H), 2.08 (t,  $J = 7.2$  Hz, 2H), 2.87 (m, 8H), 3.10 (t,  $J = 7.2$  Hz, 2H), 4.04 (s, 2H), 7.26 (d,  $J = 8.4$  Hz, 2H), 7.42 (d,  $J = 8.4$  Hz, 2H).  $^{13}\text{C}$  NMR ( $\text{CDCl}_3$ )  $\delta$  30.48, 30.52, 35.51, 126.41, 126.43, 129.88, 129.90, 168.31, and 175.60. Anal. ( $\text{C}_{25}\text{H}_{46}\text{Br}_2\text{N}_4\text{O}_3$ ) C, H, N.

**16-*N*-[4-(*tert*-Butyl)benzyl]amino-9-oxo-10,14-diazaoctadecanohydroxamic Acid Dihydrobromide (18)**

$^1\text{H}$  NMR ( $\text{CDCl}_3$ )  $\delta$  1.14 (m, 13H), 1.58 (m, 5H), 1.59 (m, 5H), 1.70 (m, 2H), 1.99 (m, 2H), 2.08 (m, 2H), 2.89 (m, 8H), 3.11 (m, 2H), 4.05 (s, 2H), 7.27 (d,  $J = 8.4$  Hz, 2H), 7.42 (d,  $J = 8.4$  Hz, 2H).  $^{13}\text{C}$  NMR ( $\text{CDCl}_3$ )  $\delta$  22.80, 24.88, 28.02, 30.50, 35.96, 45.17, 47.05, 126.42, 129.89. Anal. ( $\text{C}_{27}\text{H}_{50}\text{Br}_2\text{N}_4\text{O}_3$ ) C, H, N.

**15-*N*-[4-(*tert*-Butyl)benzyl]amino-7-*N*-{[4-*N,N*-(dimethyl)aminobenzyl] amino}-6-oxo-7,11-diazapentadecanohydroxamic Acid Dihydrobromide (19)**

$^1\text{H}$  NMR ( $\text{CDCl}_3$ )  $\delta$  1.27 (s, 9H), 1.33 (m, 8H), 1.62 (m, 6H), 2.22 (m, 4H), 2.30 (m, 6H), 2.57 (m, 12H), 3.01 (m, 4H), 3.19 (m, 4H), 4.07 (s, 2H), 4.68 (d,  $J = 5.6$  Hz, 2H), 6.87 (m, 2H), 6.95 (d,  $J = 5.6$  Hz, 4H), 7.25 (m, 4H), 7.40 (d,  $J = 8.0$  Hz, 2H), 7.79 (d,  $J = 8.0$  Hz, 2H), 7.99 (d,  $J = 7.6$  Hz, 4H). Anal. ( $\text{C}_{33}\text{H}_{55}\text{Br}_2\text{N}_5\text{O}_3$ ) C, H, N.

**17-Amino-9-*N*-{[4-*N,N*-(dimethyl)aminobenzyl]amino}-8-oxo-9,13-diazaheptadecanohydroxamic Acid Dihydrobromide (20)**

$^1\text{H}$  NMR ( $\text{CDCl}_3$ )  $\delta$  1.11 (m, 6H), 1.26 (m, 4H), 1.52 (m, 4H), 1.73 (m, 1H), 1.82 (m, 1H), 2.19 (m, 2H), 2.81 (m, 6H), 3.01 (s, 6H), 3.22 (m, 2H), 7.22 (m, 2H), 7.39 (m, 2H).  $^{13}\text{C}$  NMR ( $\text{CDCl}_3$ )  $\delta$  22.91, 24.02, 25.12, 27.22, 28.29, 32.4, 32.55, 38.89, 46.51, 115.11, 120.99, 121.00, 128.51, 128.67, 130.12, 139.25, 142.11, 179.23. IR ( $\text{cm}^{-1}$ ): 3407.6, 2940.8, 2860.3, 1712.1, 1615.3, 1514.0. Anal. ( $\text{C}_{24}\text{H}_{45}\text{Br}_2\text{N}_5\text{O}_3$ ) C, H, N.

**4-[[*N*-(*tert*-Butyloxycarbonyl)amino]methyl]benzoic Acid (25)**

A mixture of 2.0 g (0.013 mol) of **24** in 100 mL of dioxane/1.0 N sodium hydroxide (2:1) was cooled in an ice bath with stirring. To this mixture a 3.16 g (0.0015 mol) portion of di-*tert*-butyl dicarbonate was added, and the mixture was allowed to stir for 12 h at room temperature. The dioxane was removed, and the pH of the resulting aqueous solution was adjusted to 3.0 using 1.0 N HCl. The aqueous layer was extracted with three 50 mL portions of ethyl acetate, and the organic layers were combined, washed with brine, and dried over anhydrous magnesium sulfate. Filtration and removal of the solvent under reduced pressure afforded the crude *N*-Boc protected intermediate, which was purified on a silica gel column using ethyl acetate/hexane (3:4) followed by ethyl acetate/hexane (3:1). The pure compound was obtained as fine white powder (2.12 g) in 63.8% yield.  $^1\text{H}$  NMR ( $\text{CDCl}_3$ )  $\delta$  1.44 (s, 9H), 4.40 (s, 2H) 7.39 (d,  $J = 8.4$  Hz, 2H), 8.08 (d,  $J = 8.0$  Hz, 2H).  $^{13}\text{C}$  NMR ( $\text{CDCl}_3$ ) 28.59, 44.59, 127.45, 128.56, 130.76, 135.37, 171.41.

A 0.60 g (0.0024 mol) portion of the *N*-Boc protected intermediate above was dissolved in 10.0 mL of dichloromethane and cooled to 0 °C, and 1-(3-dimethylaminopropyl)-3-ethylcarbodiimide hydrochloride (EDCI, 0.503 g, 0.0026 mol) and *N*-hydroxybenzotriazole (HOBt, 0.35 g, 0.0026 mol) were added with stirring. The mixture was allowed to stir for 15 min at 0 °C, after which time 0.26 mL (0.19 mL, 0.0026 mol) of triethylamine was added. The reaction mixture was stirred for an additional 15 min at 0 °C, and then a 0.360 g portion (0.0026 mol) of *o*-nitroaniline dissolved in 2 mL of dichloromethane was added, followed by stirring for 8 h at room temperature. The reaction mixture was then concentrated in vacuo



to yield a dark-yellow semisolid. The semisolid was dissolved in 50 mL of water and extracted with three 50 mL portions of chloroform, and the combined organic layers were dried over anhydrous magnesium sulfate. Filtration and removal of the solvent then afforded crude **25**, which was purified by column chromatography (hexane/ethyl acetate 3:1) to yield pure **25** as yellow crystals (0.68 g, 76.7%). <sup>1</sup>H NMR (CDCl<sub>3</sub>) δ 1.47(s, 9H) 4.43 (d, d, *J*= 6.0 Hz, 2H), 5.56 (s, 1H), 7.48 (m, 5H), 8.06 (d, *J*= 8.4 Hz, 1H), 8.19 (d, *J*= 8.0 Hz, 2H).

### 17-*N*-[4-(*tert*-Butyl)benzyl]amino-1-*N*-[4-(*N*-(2-aminophenyl) benzamido)methyl]amino-1,5-dioxo-6,10-diazatetradecanamide Dihydrobromide (**21**)

Compound **21** was synthesized from **25** and **26** using methodology described by our laboratory<sup>7</sup> and a previously published benzamide synthesis.<sup>14,15</sup> In our hands, these syntheses provided **21** but in poor overall yield. Thus, the complete experimental details are not described in this manuscript. An improved synthesis used to produce **22** and **23** is described below. <sup>1</sup>H NMR (D<sub>2</sub>O) δ (ppm) 1.14 (s, 9H), 1.59–1.90 (complex m, 10H), 2.99 (m, 10H), 3.53 (s, 1H), 3.61 (s, 1H), 4.04 (s, 2H), 6.81 (m, 2H), 7.23 (m, 4H), 7.41 (m, 2H), 7.66 (m, 4H). Anal. (C<sub>37</sub>H<sub>54</sub>Br<sub>2</sub>N<sub>6</sub>O<sub>3</sub>) C, H, N.

### 2-[*N*-(*tert*-Butyloxycarbonyl)amino]aniline (**28**)

A 1.0 g portion of benzene-1,2-diamine **27** (0.009 mol) was dissolved in 30 mL of chloroform, and the reaction mixture was cooled to 0 °C. To this mixture was added an aqueous solution of sodium bicarbonate (0.78 g, 0.0054 mol) and sodium chloride (0.54 g, 0.00092 mol), and the mixture was allowed to stir at 0 °C for 30 min. Di-*tert*-butyl dicarbonate (2.018, 0.0092 mol) was dissolved in 20 mL of chloroform, and the solution was slowly added to the mixture. The mixture was allowed to stir at 0 °C for an additional 10 min, warmed to room temperature, and then refluxed for 12 h. The mixture was then cooled to room temperature and extracted with three 30 mL portions of chloroform. The combined organic layers were washed with 50 mL of saturated sodium bicarbonate and 50 mL of saturated sodium chloride solution and then dried over anhydrous magnesium sulfate. The combined organic layers were then filtered, and the solvent was removed in vacuo to yield crude **28**. The crude compound was purified on a silica gel column eluted with hexane/ethyl acetate (3:1, then 2:1) to yield compound **28** as an off-white solid (1.55 g, 80.1%). <sup>1</sup>H NMR (CDCl<sub>3</sub>) δ 1.51 (s, 9H), 3.73 (br, 2H), 6.21 (br, 1H), 6.78 (m, 2H), 7.01 (m, 1H), 7.28 (d, *J*= 9.2 Hz, 1H). <sup>13</sup>C NMR (CDCl<sub>3</sub>) δ 28.0, 29.9, 116, 124, 127, 129.4, 129.9, 158. IR (cm<sup>-1</sup>) 3435, 1735.

### 17-{*N*-[4-(*tert*-Butyl)benzyl]-*N*-[2-(mesitylene)sulfonyl]}amino-13-*N*-[2-(mesitylene)sulfonyl]-1-*N*-[4-(carboxy)benzyl]amino-1,8-dioxo-9,13-diazaheptadecanamide Methyl Ester (**31a**)

A 0.341 g (0.00042 mol) of **30a** was dissolved in 3 mL of dichloromethane, and to this mixture was added 2 mL of dichloromethane containing **29** (0.08 g, 0.0005 mol), HOBT (0.067 g, 0.0005 mol), and triethylamine (0.050 g, 0.0007 mol). The reaction mixture was cooled to 0 °C, and 1-ethyl-3-(3-dimethylaminopropyl)carbodiimide (EDCI) (0.163 g, 0.00085 mol) was added in 5 mL of dichloromethane. Following the addition of EDCI, the resulting mixture was stirred at 0 °C for 10 additional min, and the mixture was allowed to warm to room temperature and stirred for 12 h. The resulting dichloromethane solution was washed with 20 mL of 0.5 M HCl, 20 mL of water, and 20 mL of saturated NaHCO<sub>3</sub>. The organic layer was dried over anhydrous magnesium sulfate and filtered, and the dichloromethane was removed under reduced pressure. The crude product was purified by column chromatography (hexane/ethyl acetate 2:1, then 1:2) to yield **31a** as a white solid (0.383 g, 95.3%) <sup>1</sup>H NMR (CDCl<sub>3</sub>) δ 1.27 (m, 4H), 1.32 (s, 9H), 1.37 (m, 4H), 1.53 (m, 4H), 1.70 (m, 2H), 2.19–2.25 (m, 4H), 2.37 (s, 3H), 2.61 (s, 6H), 3.13–3.24 (m, 6H), 3.44 (t,

2H), 3.76 (s, 3H), 4.29 (s, 2H), 4.83 (s, 2H), 7.14–7.37 (m, 8H), 7.74–8.0 (m, 3H), 8.39 (m, 1H).  $^{13}\text{C}$  NMR ( $\text{CDCl}_3$ )  $\delta$  21.9, 22.8, 25.2, 28.2, 31.9, 37.1, 43.9, 47.7, 48.2, 48.7, 52.5, 53.7, 128.8, 129.7, 133.4, 137.6, 142.9, 144.6, 172.0, 172.7.

**17-{*N*-[3,3-(Diphenyl)propyl]-*N*-[2-(mesitylene)sulfonyl]}amino-13-*N*-[2-(mesitylene)sulfonyl]-1-*N*-[4-(carboxy)benzyl]amino-1,8-dioxo-9,13-diazaheptadecanamide Methyl Ester (31b)**

Compound **31b** was synthesized from **30b** and **29** exactly as described for the synthesis of **31a** in 92.4% yield.  $^1\text{H}$  NMR ( $\text{CDCl}_3$ )  $\delta$  1.25–1.37 (m, 10H), 1.55–1.67 (m, 6H), 1.98–2.08 (m, 4H), 2.20 (s, 3H), 2.31 (s, 3H), 2.43 (s, 6H), 2.56 (s, 6H), 2.90 (q,  $J = 6$  Hz, 2H), 3.05 (m, 2H), 3.15–3.22 (m, 6H), 3.66 (m, 1H), 3.906 (s, 3H), 4.14–4.46 (m, 2H), 5.96 (t, 1H), 6.32 (t, 1H), 6.90 (m, 4H), 7.00 (m, 4H), 7.12–7.21 (m, 6H), 7.29–7.36 (m, 2H), 7.96–8.00 (m, 2H).  $^{13}\text{C}$  NMR ( $\text{CDCl}_3$ )  $\delta$  21.16, 22.91, 23.08, 24.46, 24.72, 25.67, 28.82, 28.91, 29.91, 32.74, 36.42, 36.59, 36.71, 43.26, 44.09, 45.29, 45.79, 48.86, 52.32, 126.65, 127.63, 127.70, 128.79, 130.10, 130.16, 132.25, 132.31, 133.35, 140.22, 142.64, 142.83, 143.83, 144.13, 167.08, 173.46. IR ( $\text{cm}^{-1}$ ) 3386, 3295, 2969, 2843, 1721, 1652, 1543, 1313, 1147, 913, 730.

**17-{*N*-[4-(*tert*-Butyl)benzyl]-*N*-[2-(mesitylene)sulfonyl]}amino-13-*N*-[2-(mesitylene)sulfonyl]-1-*N*-[4-(carboxy)benzyl]amino-1,8-dioxo-9,13-diazaheptadecanamide (32a)**

A 0.383 g (0.0004 mol) portion of **31a** was dissolved in 12 mL of tetrahydrofuran:water (4:2) and cooled to 0 °C, and 6 mL of 1.0 N LiOH was added to the mixture dropwise. The solution was warmed to room temperature and allowed to stir for 16 h, during which time the reaction was monitored by TLC. The mixture was again cooled to 0 °C, neutralized by the dropwise addition of 2.0 N HCl, and extracted with three 20 mL portions of ethyl acetate. The ethyl acetate layers were combined, washed with brine, and dried over anhydrous magnesium sulfate. Removal of the solvent in vacuo yielded compound **32a** as a cloudy yellow oil (0.372 g, 98.4%) that was of sufficient purity to be used in the next reaction without further purification.  $^1\text{H}$  NMR ( $\text{CDCl}_3$ )  $\delta$  1.22 (m, 4H), 1.33 (s, 9H), 1.41 (m, 4 h), 1.49 (m, 4H), 1.72 (q, 2H), 2.20 (m, 4H), 2.34 (s, 6H), 2.66 (s, 12H), 3.08 (m, 6H), 3.39 (t, 2H), 4.29 (s, 2H), 4.37 (s, 2H), 7.09 (m, 2H), 7.19 (m, 4H), 7.37 (m, 2H), 7.54 (m, 2H), 7.68 (m, 1H), 7.99 (m, 2H), 8.27 (m, 1H).

**17-{*N*-[3,3-(Diphenyl)propyl]-*N*-[2-(mesitylene)sulfonyl]}amino-13-*N*-[2-(mesitylene)sulfonyl]-1-*N*-[4-(carboxy)benzyl]amino-1,8-dioxo-9,13-diazaheptadecanamide (32b)**

Compound **32b** was made from **31b** exactly as described for the synthesis of **32a** in 98.1% yield.  $^1\text{H}$  NMR ( $\text{CDCl}_3$ )  $\delta$  1.28–1.33 (m, 10H), 1.56–1.64 (m, 6H), 2.01 (q,  $J = 7.6$  Hz, 2H), 2.10 (t,  $J = 7.6$  Hz, 2H), 2.25 (s, 3H), 2.32 (s, 3H), 2.43 (s, 6H), 2.53 (s, 6H), 2.91 (t,  $J = 8$  Hz, 2H), 3.08 (m, 4H), 3.06–3.16 (m, 4H), 3.72 (t,  $J = 7.6$  Hz, 1H), 4.40 (s, 2H), 6.0 (br, 1H), 6.97 (d,  $J = 8.0$  Hz, 4H), 7.04 (d,  $J = 8.0$  Hz, 4H), 7.14 (m, 2H), 7.18 (m, 4H), 7.33 (m, 2H), 7.68 (t, 1H), 7.94 (m, 2H).  $^{13}\text{C}$  NMR ( $\text{CDCl}_3$ )  $\delta$  21.00, 21.16, 22.83, 23.05, 25.43, 25.58, 28.59, 29.91, 32.80, 36.47, 43.37, 43.60, 48.68, 102.29, 126.65, 127.60, 127.76, 128.79, 130.61, 132.29, 132.36, 133.07, 140.25, 142.94, 143.73, 174.07, 174.29, 176.96.

**17-{*N*-[4-(*tert*-Butyl)benzyl]-*N*-[2-(mesitylene)sulfonyl]}amino-13-*N*-[2-(mesitylene)sulfonyl]-1-*N*-[4-(*N*-(2-aminophenyl)benzamido)methyl]amino-1,8-dioxo-9,13-diazaheptadecanamide (33a)**

Compound **33a** was synthesized from **32a** and **28** using the procedure described for the synthesis of **31a** in 80.7% yield.  $^1\text{H}$  NMR ( $\text{CDCl}_3$ )  $\delta$  1.27 (s, 9H), 1.33 (m, 8H), 1.62 (m, 6H), 2.22 (m, 4H), 2.30 (m, 6H) 2.57 (m, 12H), 3.01 (m, 4H), 3.19 (m, 4H), 4.07 (s, 2H),

4.18 (d,  $J = 5.6$  Hz, 2H), 6.87 (m, 2H), 6.95 (d,  $J = 5.6$  Hz, 4H), 7.25 (m, 4H), 7.40 ( $J = 7.8$  Hz, 2H), 7.99 (d,  $J = 7.6$  Hz, 4H).

**17-*N*-[3,3-(Diphenyl)propyl]-*N*-[2-(mesitylene)sulfonyl]amino-13-*N*-[2-(mesitylene)sulfonyl]-1-*N*-[4-(*N*-(2-aminophenyl)benzamido)methyl]amino-1,8-dioxo-9,13-diazaheptadecanamide (33b)**

Compound **33b** was synthesized from **32b** and **28** using the procedure described for the synthesis of **31a** in 84.2% yield.  $^1\text{H}$  NMR ( $\text{CDCl}_3$ )  $\delta$  1.37 (m, 8H), 1.49–1.53 (m, 11H), 1.64 (m, 4H), 2.04 (m, 6H), 2.21 (s, 3H), 2.31 (s, 3H), 2.43 (s, 6H), 2.54 (s, 6H), 2.90 (t,  $J = 8$  Hz, 2H), 2.92 (t,  $J = 8$  Hz, 2H), 3.13–3.20 (m, 6H), 3.64 (t,  $J = 7.6$  Hz, 1H), 4.45 (d,  $J = 6$  Hz, 2H), 6.05 (broad s, 1H), 2.65 (broad s, 1H), 6.90 (d,  $J = 5.6$  Hz, 2H), 6.98 (d,  $J = 5.6$  Hz, 4H), 7.14–7.31 (m, 12H), 7.31 (m, 1H), 7.65 (m, 1H), 7.89 (d,  $J = 8$  Hz, 2H), 9.4 (br, 1H).  $^{13}\text{C}$  NMR (400 MHz  $\text{CDCl}_3$ )  $\delta$  14.14, 21.19, 22.91, 23.08, 24.42, 25.72, 28.52, 28.86, 36.54, 43.19, 44.07, 45.17, 48.84, 125.70, 126.65, 127.63, 127.89, 128.03, 128.79, 132.27, 132.32, 140.21, 140.19, 142.66, 143.12, 143.78, 173.69, 183.70. IR ( $\text{cm}^{-1}$ ) 3439, 3021, 2921, 2843, 1652, 1526, 1313, 1213, 1095, 850.

**17-*N*-[4-(*tert*-Butyl)benzyl]amino-1-*N*-[4-(*N*-(2-aminophenyl) benzamido)methyl]amino-1,8-dioxo-9,13-diazaheptadecanamide Dihydrobromide (22)**

A 4.2 g portion of phenol (0.44 mol) was dissolved in 20 mL of 30% HBr in acetic acid in a stoppered flask. Compound **33a** (0.200 g, 0.0002 mol) in 15 mL of ethyl acetate was then added in three portions over a period of 3 h. After the addition was complete, the reaction mixture was stirred for an additional 15 h at room temperature, then cooled to 0 °C and diluted with 30 mL of water. The aqueous phase was washed with two 30 mL portions of ethyl acetate before being lyophilized to give the crude product as yellow solid. This crude product was washed with methanol and filtered to yield the tetrahydrobromide salt of **22** (0.099 g, 74.2%) as an off-white solid. An analytical sample of **22** was prepared by recrystallization from aqueous ethanol.  $^1\text{H}$  NMR ( $\text{D}_2\text{O}$ )  $\delta$  1.15 (s, 9H), 1.21 (m, 4H), 1.34–1.71 (m, 10H), 1.97 (t, 1H), 2.11 (m, 3H), 2.85 (m, 6H), 3.07 (m, 2H), 3.97 (s, 1H), 4.05 (s, 1H), 4.23 (m, 2H), 7.19 (d,  $J = 8$  Hz, 2H), 7.24–7.34 (m, 4H), 7.44 (m, 2H), 7.61 (d,  $J = 8$  Hz, 2H), 7.84 (d,  $J = 7.6$  Hz, 2H). Anal. ( $\text{C}_{40}\text{H}_{60}\text{Br}_2\text{N}_6\text{O}_3$ ) C, H, N.

**17-*N*-[3,3-(Diphenyl)propyl]amino-1-*N*-[4-(*N*-(2-aminophenyl)benzamido)methyl]amino-1,8-dioxo-9,13-diazaheptadecanamide Dihydrobromide (23)**

Compound **23** was prepared from **33b** exactly as described for the synthesis of **22** in 76.7% yield. An analytical sample of **23** was prepared by recrystallization from aqueous ethanol.  $^1\text{H}$  NMR ( $\text{D}_2\text{O}$ )  $\delta$  1.12 (m, 4H), 1.20 (m, 4H), 1.53 (m, 4H), 1.69 (m, 2H), 2.01 (t,  $J = 7.2$  Hz, 2H), 2.14 (m, 2H), 2.32 (m, 2H), 2.70–2.84 (m, 8H), 3.09 (t,  $J = 7.2$  Hz, 2H), 3.95 (t,  $J = 7.2$  Hz, 1H), 4.29 (s, 2H), 6.64 (d,  $J = 8.8$  Hz, 1H), 6.83 (d,  $J = 8.8$  Hz, 1H), 6.80 (m, 1H), 6.98 (m, 1H), 7.13 (m, 2H), 7.26 (m, 6H), 7.34 (m, 4H), 7.77 (d,  $J = 8$  Hz, 2H).  $^{13}\text{C}$  NMR ( $\text{D}_2\text{O}$ )  $\delta$  16.92, 20.52, 22.73, 22.83, 25.35, 25.75, 27.95, 28.07, 30.86, 35.71, 35.79, 35.89, 42.79, 45.06, 46.37, 46.72, 46.90, 48.06, 57.58, 113.83, 115.49, 117.48, 121.42, 126.64, 127.12, 127.58, 128.19, 128.65, 129.16, 129.22, 130.13, 130.31, 132.61, 143.58, 144.54, 176.85, 177.44, 177.82. IR ( $\text{cm}^{-1}$ ) 3408, 2934, 2847, 1469, 1378. Anal. ( $\text{C}_{44}\text{H}_{60}\text{Br}_2\text{N}_6\text{O}_3$ ) C, H, N.

**Histone Deacetylase Activity Assay**

Compounds **6–23** were evaluated for their ability to inhibit isolated HDAC in a commercially available assay (Fluor de Lys assay system, Biomol International LP, Plymouth Meeting, PA), employing **1** and **2** as positive controls.<sup>8</sup> The reaction mixture contains a HeLa cell nuclear extract and a commercial substrate containing acetylated lysine

side chains. The substrate and extract are incubated in the presence of the appropriate concentration of the inhibitor. Deacetylation of the substrate followed by mixing with the provided developer generates a fluorophore, and comparison of inhibited vs control relative fluorescence using a standard plate reader was employed to determine percent HDAC activity remaining. For studies involving individually expressed HDACs 3 and 6, the appropriate HDAC protein was purchased from BPS Bioscience (San Diego, CA), and a comparable solution of the pure isoform was substituted for the HeLa cell assay in the Fluor de Lys kit. All determinations were carried out in triplicate, and reported values are the average of these determinations, which in no case varied by more than 3%.

### Cell Lines and Drug Treatment

HCT116 colon carcinoma cells were provided by Dr. Bert Vogelstein.<sup>27</sup> Cells were maintained in McCoy's 5A medium supplemented with 10% fetal calf serum, at 37 °C, 5% CO<sub>2</sub>. Seeded cells were allowed to adhere overnight, then treated with **1** (Wako Pure Chemicals, Richmond, VA), **2** (Mitsui Pharmaceuticals, Chiba, Japan), SAHA (BioVision, Mountain View, CA), or the desired test compound for the concentration and time indicated in the figure captions. For combination studies, attached cells were incubated with 0.1 μM 5-aza-dC (Sigma) for 24 h, after which medium was removed and replaced with fresh medium containing the appropriate concentration of PABA **22** for an additional 24 h.

### Histone Preparation

Histones were prepared by a modification of a previously described method.<sup>8,28</sup> Cells were washed in 2 mL of HBSS and disrupted by 1 mL of ice-cold lysis buffer A (10 mM Tris, pH 7.6, 5 mM butyric acid, 1% Triton X-100, 1 mM MgCl<sub>2</sub>, and 1 mM PMSF). Nuclei were collected by centrifugation at 14 000 rpm for 15 min. The pellet was resuspended once with 250 μL of ice-cold lysis buffer B (10 mM Tris, pH 7.6, 0.25 M sucrose, 3 mM CaCl<sub>2</sub>, and 5 mM butyric acid). Sulfuric acid was added to a concentration of 0.4 N, and the tubes were incubated at 4 °C for overnight. Debris was pelleted by centrifugation, and the supernatant was collected. Histones were precipitated by addition of 10 volumes of acetone and incubated at -20 °C overnight. Pellets were collected by centrifugation, briefly dried under vacuum, and resuspended in doubly distilled H<sub>2</sub>O.

### Protein Expression Analysis

Following treatment, HCT116 cells were lysed in buffer M (25 mM HEPES, pH 7.9, 150 mM NaCl, 0.5 mM EDTA, 0.1% Triton-X, 10% glycerol, 0.1 mg/ml BSA, 1 mM DTT) containing an EDTA-free protease inhibitor cocktail, at 4 °C for 20 min. Lysate was clarified by centrifugation at 14000g for 15 min at 4 °C, and the resulting supernatant was used for analysis. Total protein concentration was determined using the BioRad DC assay (Hercules, CA), with absorbance measured using a spectrophotometer at a wavelength of 750 nm. Absorbance was converted to protein content using a bovine serum albumin standard curve. Total cellular proteins (30 μg per lane) were separated on 10% Bis-Tris NOVEX gels (Invitrogen, Carlsbad, CA), transferred to Immunoblot PVDF membrane (BioRad), and proteins of interest were visualized by Western blot analysis using the following primary antibodies: acetylhistone H3 (06-599) (diluted 1:1000) and acetylhistone H4 (06-866) (diluted 1:1000), from Upstate Biotechnologies (Billerica, MA); p21<sup>Waf1</sup> (556431) (diluted 1:500) from BD Pharmingen (San Jose, CA); p16 (36-5600) (1:1000) from Zymed (San Francisco, CA); acetylated R-tubulin (Sigma No. T-6793) (1:2000); and  $\alpha$ -actin (sc-1615) (diluted 1:1500) from Santa Cruz (Santa Cruz, CA). Following washes, blots were incubated with species-specific, fluorophore-conjugated secondary antibodies to allow visualization and quantification of immunoreactive proteins using the Odyssey infrared detection system and software (LI-COR, Lincoln, NE).

PAHA and PABA uptake by the polyamine transporter was determined by measuring the ability of each compound to compete with the uptake of  $^{14}\text{C}$ -spermidine, as previously described.<sup>29</sup>

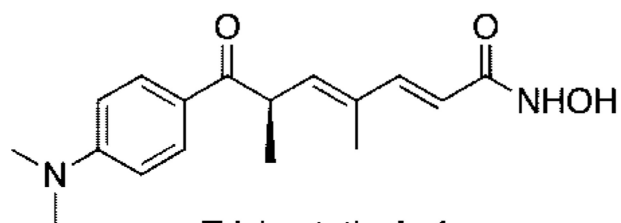
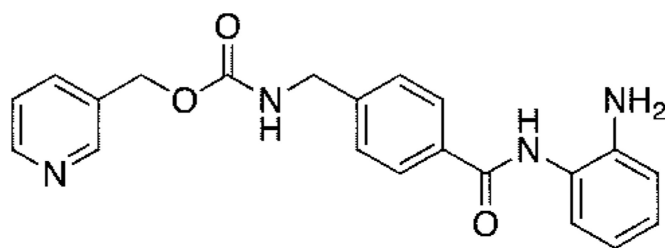
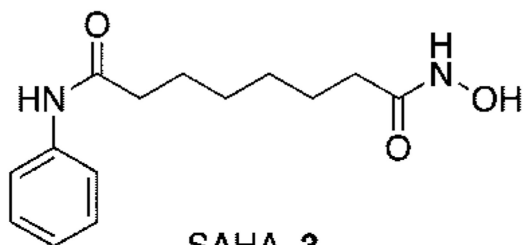
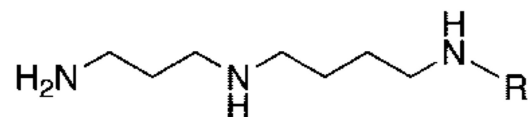
### Cytoproliferative Responses to PAHA and PABA Exposure

Cell proliferation was quantified using the CellTiter 96 One Solution MTS assay (Promega, Madison, WI). Cells were seeded in triplicate in 96-well plates at a density of 3000 cells per well and allowed to attach overnight. Medium was aspirated and replaced with 100  $\mu\text{L}$  of fresh medium containing the appropriate concentration of HDAC inhibitor, PAHA, or PABA. Following incubation at 37 °C, 5%  $\text{CO}_2$ , 20  $\mu\text{L}$  of CellTiter 96 One Solution was added per well and incubated 1.5 h at 37 °C and absorbance measured at 490 nm.

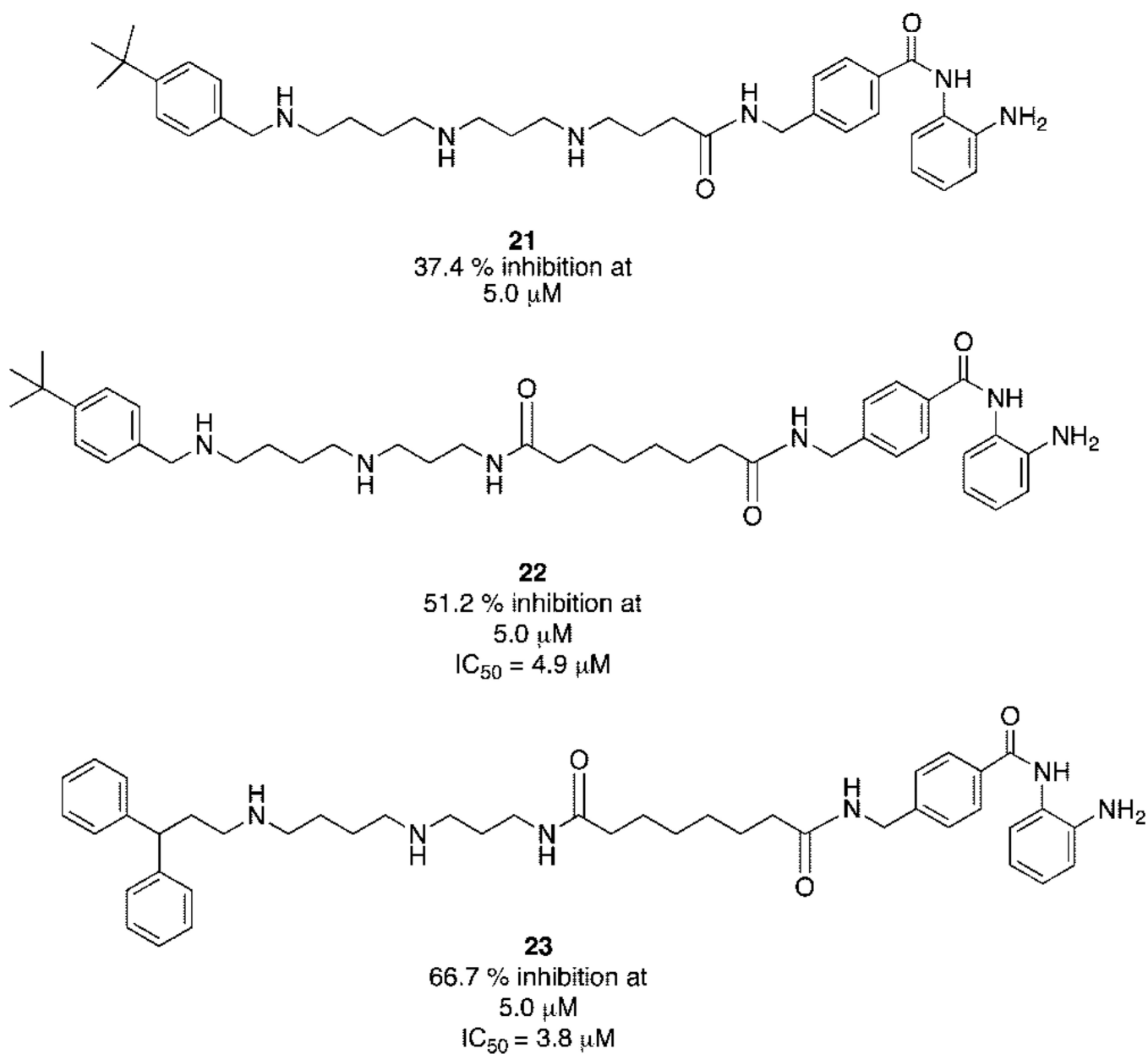
### References

1. Johnstone RW. Histone Deacetylase Inhibitors: Novel Drugs for the Treatment of Cancer. *Nat. Rev. Drug. Discovery*. 2002; 1:287–299.
2. Marks PA, Rifkind RA, Richon VM, Breslow R, Miller T, Kelly WK. Histone Deacetylases and Cancer: Causes and Therapies. *Nat. Rev. Cancer*. 2001; 1:194–202. [PubMed: 11902574]
3. Suzuki T, Ando T, Tsuchiya K, Fukazawa N. Synthesis and Histone Deacetylase Inhibitory Activity of New Benzamide Derivatives. *J. Med. Chem.* 1999; 42:3001–3003. [PubMed: 10425110]
4. Grozinger CM, Schrieber SL. Deacetylase Enzymes: Biological Functions and the Use of Small Molecule Inhibitors. *Chem. Biol.* 2002; 9:3–16. [PubMed: 11841934]
5. Weinmann H, Ottow E. Recent Advances in Medicinal Chemistry of Histone Deacetylase Inhibitors. *Annu. Rep. Med. Chem.* 2004; 39:185–196.
6. (a) For a toxicological profile of 1 and recent clinical studies involving 2 and 3, see the following: Vanhaecke T, Papeleu P, Elaut G, Rogiers V. Trichostatin A-like Hydroxamate Histone Deacetylase Inhibitors as Therapeutic Agents: Toxicological Point of View. *Curr. Med. Chem.* 2004; 11:1629–1643. [PubMed: 15180568] Fouladi M. Histone Deacetylase Inhibitors in Cancer Therapy. *Cancer Invest.* 2006; 24:521–527. [PubMed: 16939962]
7. Bieliauskas AV, Weerasinghe SVW, Plfum MKH. Structural Requirements of HDAC Inhibitors: SAHA Analogues Functionalized Adjacent to the Hydroxamic Acid. *Bioorg. Med. Chem. Lett.* 2007; 17(8):2216–2219. [PubMed: 17307359]
8. Varghese S, Gupta D, Baran T, Jiemjit A, Gore SD, Casero RA Jr, Woster PM. Alkyl Substituted Polyaminohydroxamic Acids: A Novel Class of Targeted Histone Deacetylase Inhibitors. *J. Med. Chem.* 2005; 48:6350–6365. [PubMed: 16190761]
9. Casero RA Jr, Woster PM. Terminally Alkylated Polyamine Analogues as Chemotherapeutic Agents. *J. Med. Chem.* 2001; 44:1–29. [PubMed: 11141084]
10. Valasinas A, Reddy VK, Blohkin AV, Basu HS, Bhattacharya S, Sarkar A, Marton LJ, Frydman B. Long-Chain Polyamines (Oligoamines) Exhibit Strong Cytotoxicities against Human Prostate Cancer Cells. *Bioorg. Med. Chem.* 2003; 11:4121–4131. [PubMed: 12927874]
11. Frydman B, Porter CW, Maxuitenko Y, Sarkar A, Bhattacharya S, Valasinas A, Reddy VK, Kisiel N, Marton LJ, Basu HS. A Novel Polyamine Analog (SL-11093) Inhibits Growth of Human Prostate Tumor Xenografts in Nude Mice. *Cancer Chemother. Pharmacol.* 2003; 51:488–492. [PubMed: 12695854]
12. Ha HC, Yager JD, Woster PM, Casero RA. Structural Specificity of Polyamines and Polyamine Analogues in the Protection of DNA from Strand Breaks Induced by Reactive Oxygen Species. *Biochem. Biophys. Res. Commun.* 1998; 244:298–303. [PubMed: 9514920]
13. Cullis PM, Green RE, Merson-Davies L, Travis NG. Chemical Highlights of Polyamine Transport. *Biochem. Soc. Trans.* 1998; 26:595–601. [PubMed: 10047789]
14. Wunsch E, Graf W, Keller O, Keller W, Wersin G. On the Synthesis of Benzyloxycarbonyl Amino Acids. *Synthesis*. 1986:958–960.
15. Nagaoka Y, Maeda T, Kawai Y, Nakashima D, Oikawa T, Shimoke T, Ikeuchi I, Kuwajima H, Uesato S. Synthesis and Cancer Antiproliferative Activity of New Histone Deacetylase Inhibitors:

- Hydrophilic Hydroxamates and 2-Aminobenzamide-Containing Derivatives. *Eur. J. Med. Chem.* 2006; 41:697–708. [PubMed: 16584813]
16. Bamford MJ, Alberti MJ, Bailey N, Davies S, Dean DK, Gaiba A, Garland S, Harling JD, Jung DK, Panchal TA, Parr CA, Steadman JG, Takle AK, Townsend JT, Wilson DM, Witherington J. (1*H*-Imidazo[4,5-*c*]pyridin-2-yl)-1,2,5-oxadiazol-3-ylamine Derivatives: A Novel Class of Potent MSK-1 Inhibitors. *Bioorg. Med. Chem. Lett.* 2005; 15:3402–3406. [PubMed: 15950465]
  17. Lu Q, Yang YT, Chen CS, Davis M, Byrd JC, Etherton MR, Umar A, Chen CS. Zn<sup>2+</sup>-Chelating Motif-Tethered Short-Chain Fatty Acids as a Novel Class of Histone Deacetylase Inhibitors. *J. Med. Chem.* 2004; 47:467–474. [PubMed: 14711316]
  18. Yajima H, Takeyama M, Kanaki J, Nishimura O, Fujino M. Studies on Peptides. LXXX. NG-Mesitylene-2-sulfonylarginine. *Chem. Pharm. Bull.* 1978; 26:3752–3757.
  19. Roemmele RC, Rapoport H. Removal of *N*-Arylsulfonyl Groups from Hydroxy R-Amino Acids. *J. Org. Chem.* 1988; 53:2367–2371.
  20. Belting M, Mani K, Jonsson M, Cheng F, Sandgren S, Jonsson S, Ding K, Delcros JG, Fransson LA. Glypican-1 Is a Vehicle for Polyamine Uptake in Mammalian Cells: A Pivotal Role for Nitrosothiol-Derived Nitric Oxide. *J. Biol. Chem.* 2003; 278:47181–47189. [PubMed: 12972423]
  21. Soulet D, Gagnon B, Rivest S, Audette M, Poulin R. A Fluorescent Probe of Polyamine Transport Accumulates into Intracellular Acidic Vesicles via a Two-Step Mechanism. *J. Biol. Chem.* 2004; 279:49355–49366. [PubMed: 15208319]
  22. Kouraklis G, Theocharis S. Histone Deacetylase Inhibitors: A Novel Target of Anticancer Therapy. *Oncol. Rep.* 2006; 15:489–494. [PubMed: 16391874]
  23. Ryan QC, Headlee D, Acharya M, Sparreboom A, Trepel JB, Joseph Ye J, Figg WD, Hwang K, Chung EJ, Murgo A, Melillo G, Elsayed Y, Monga M, Kalnitskiy M, Zwiebel J, Sausville EA. Phase I and Pharmacokinetic Study of MS-275, a Histone Deacetylase Inhibitor, in Patients with Advanced and Refractory Solid Tumors or Lymphoma. *J. Clin. Oncol.* 2005; 23:3912–3922. [PubMed: 15851766]
  24. Cameron EE, Baylin SB, Herman JG. p15(INK4B) CpG Island Methylation in Primary Acute Leukemia Is Heterogeneous and Suggests Density as a Critical Factor for Transcriptional Silencing. *Blood.* 1999; 94:2445–2451. [PubMed: 10498617]
  25. Corn PG, Smith BD, Ruckdeschel ES, Douglas D, Baylin SB, Herman JG. E-Cadherin Expression Is Silenced by 5' CpG Island Methylation in Acute Leukemia. *Clin. Cancer Res.* 2000; 6:4243–4248. [PubMed: 11106238]
  26. Seiler N, Delcros JG, Moulinoux JP. Polyamine Transport in Mammalian Cells. An Update. *Int. J. Biochem. Cell Biol.* 1996; 28:843–861. [PubMed: 8811834]
  27. Bunz F, Fauth C, Speicher MR, Dutriaux A, Sedivy JM, Kinzler KW, Vogelstein B, Lengauer C. Targeted Inactivation of p53 in Human Cells Does Not Result in Aneuploidy. *Cancer Res.* 2002; 62:1129–1133. [PubMed: 11861393]
  28. Cousens LS, Gallwitz D, Alberts BM. Different Accessibilities in Chromatin to Histone Acetylase. *J. Biol. Chem.* 1979; 254:1716. [PubMed: 762168]
  29. Aziz SW, Yatin M, Worthen DR, Lipke DW, Crooks PA. A Novel Technique for Visualizing the Intracellular Localization and Distribution of Transported Polyamines in Cultured Pulmonary Artery Smooth Muscle Cells. *J. Pharm. Biol. Anal.* 1998; 17:307–320.

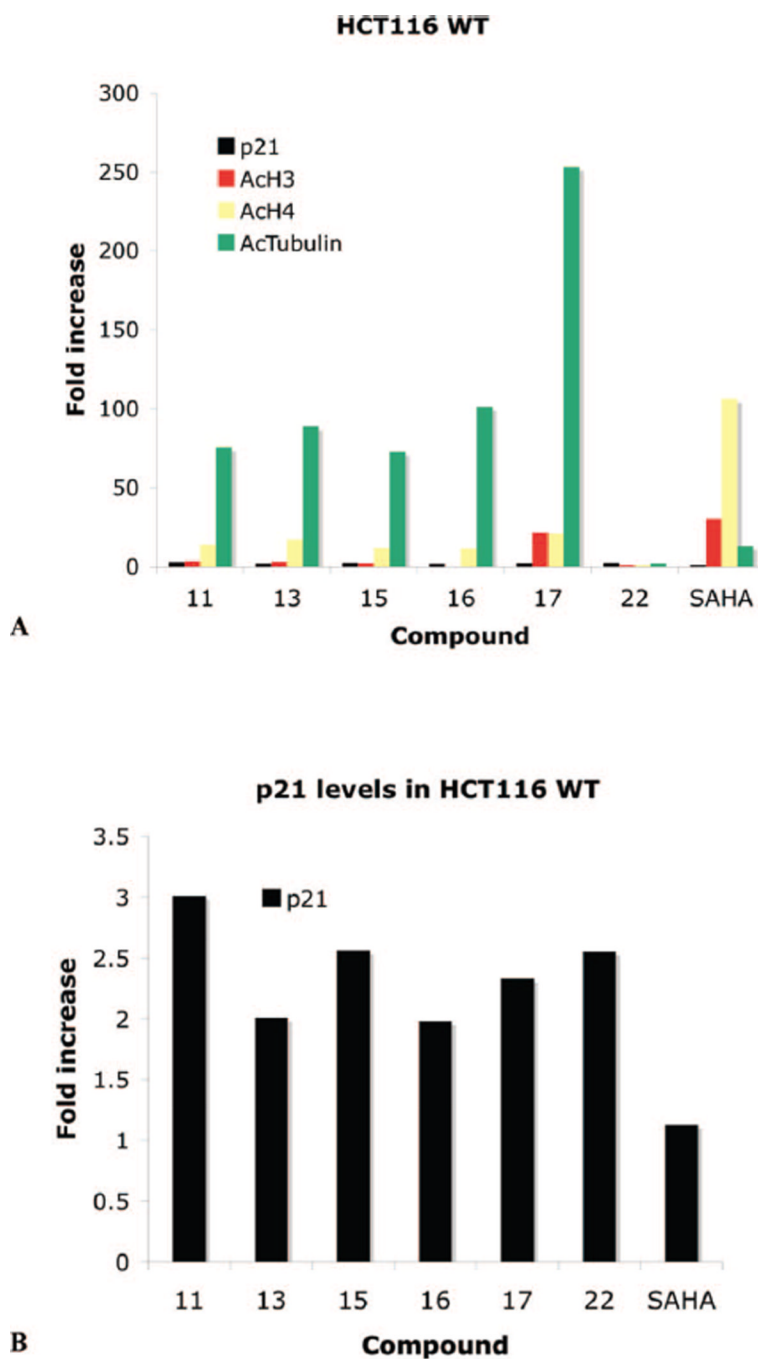
Trichostatin A, **1****2**SAHA, **3**spermidine, **4** (R = H)  
spermine, **5** (R = aminopropyl)

**Figure 1.**  
Structures of **1** (trichostatin A), **2**, **3** (SAHA), **4** (spermidine), and **5** (spermine).

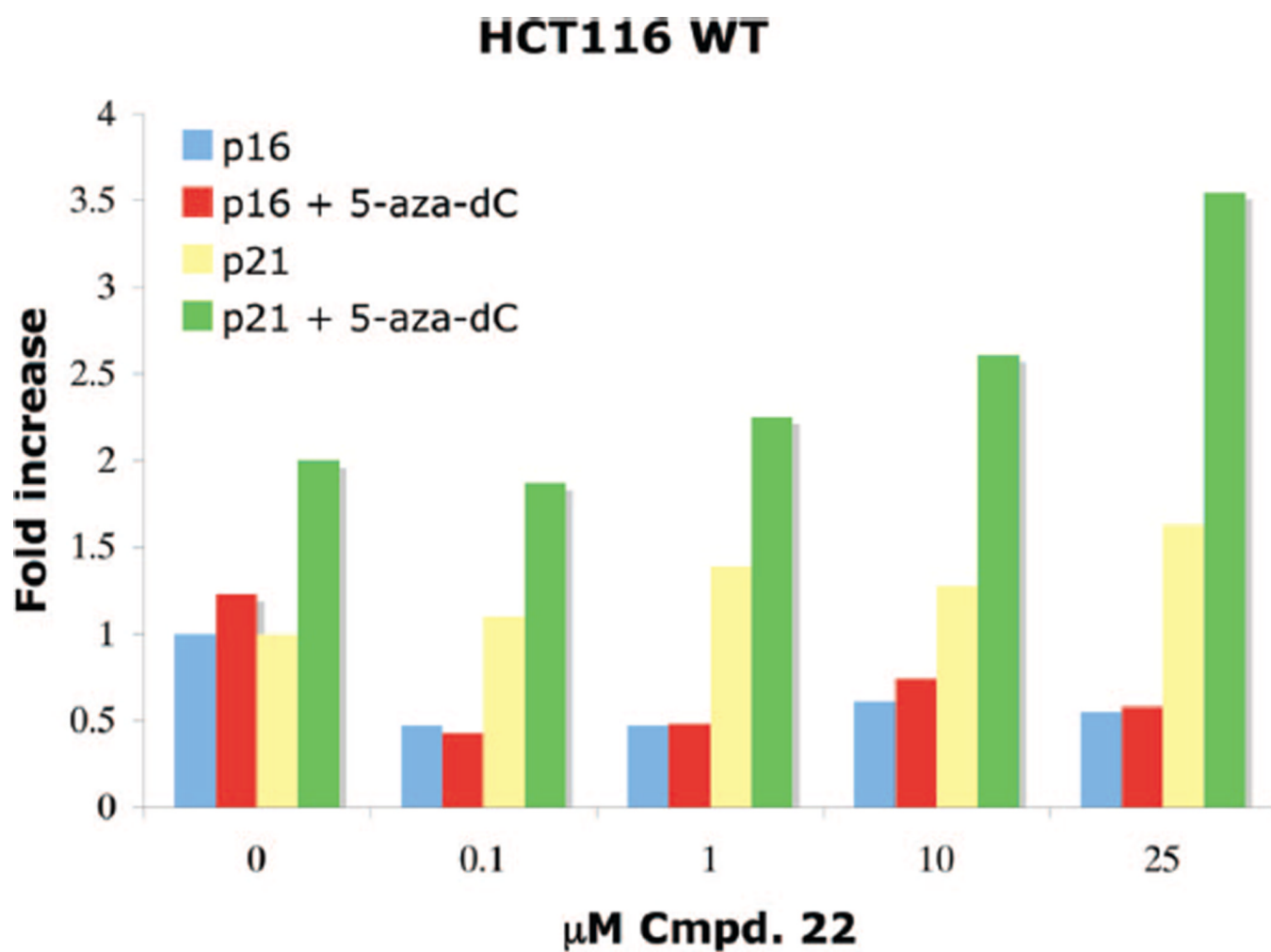


**Figure 2.** Structures of PABA analogues **21–23** and their inhibitory activity against histone deacetylase at 5.0  $\mu\text{M}$ . Percent inhibition values reported are the average of three determinations that in all cases differed by 5% or less.



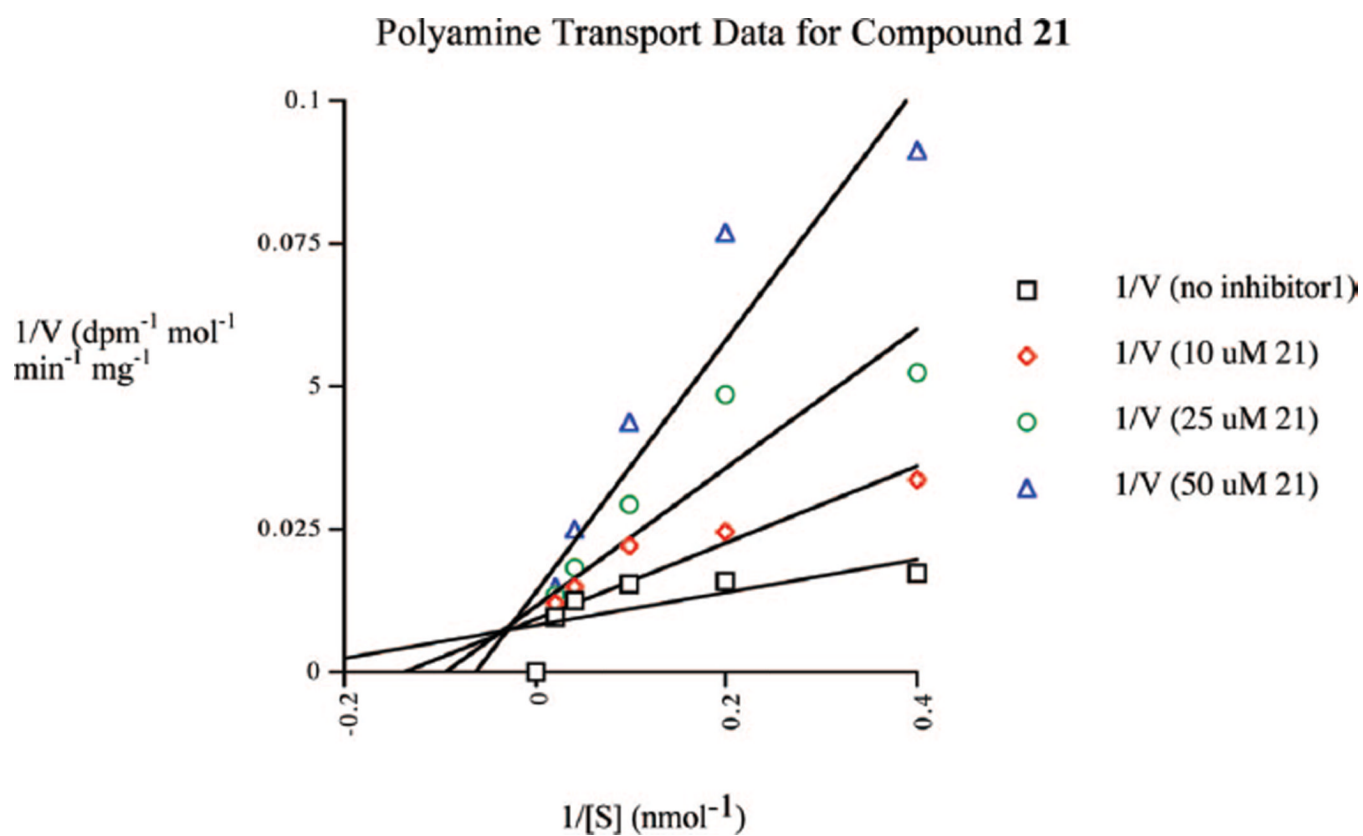


**Figure 3.** Fold increase in the re-expression of p21<sup>Waf1</sup>, acetylated histones H3 (AcH3) and H4 (AcH4), and acetylated R-tubulin (AcTub) proteins in HCT116 colon carcinoma cells. Cells were treated for 24 h with 10  $\mu$ M compounds **11**, **13**, **15**, **16**, **18**, **22**, and SAHA: (A) p21, AcH3, AcH4, and AcTub values in the HCT166 cell line; (B) amplification of p21 data from part A. Data points are single determinations derived from infrared detection and quantification of representative Western blots.

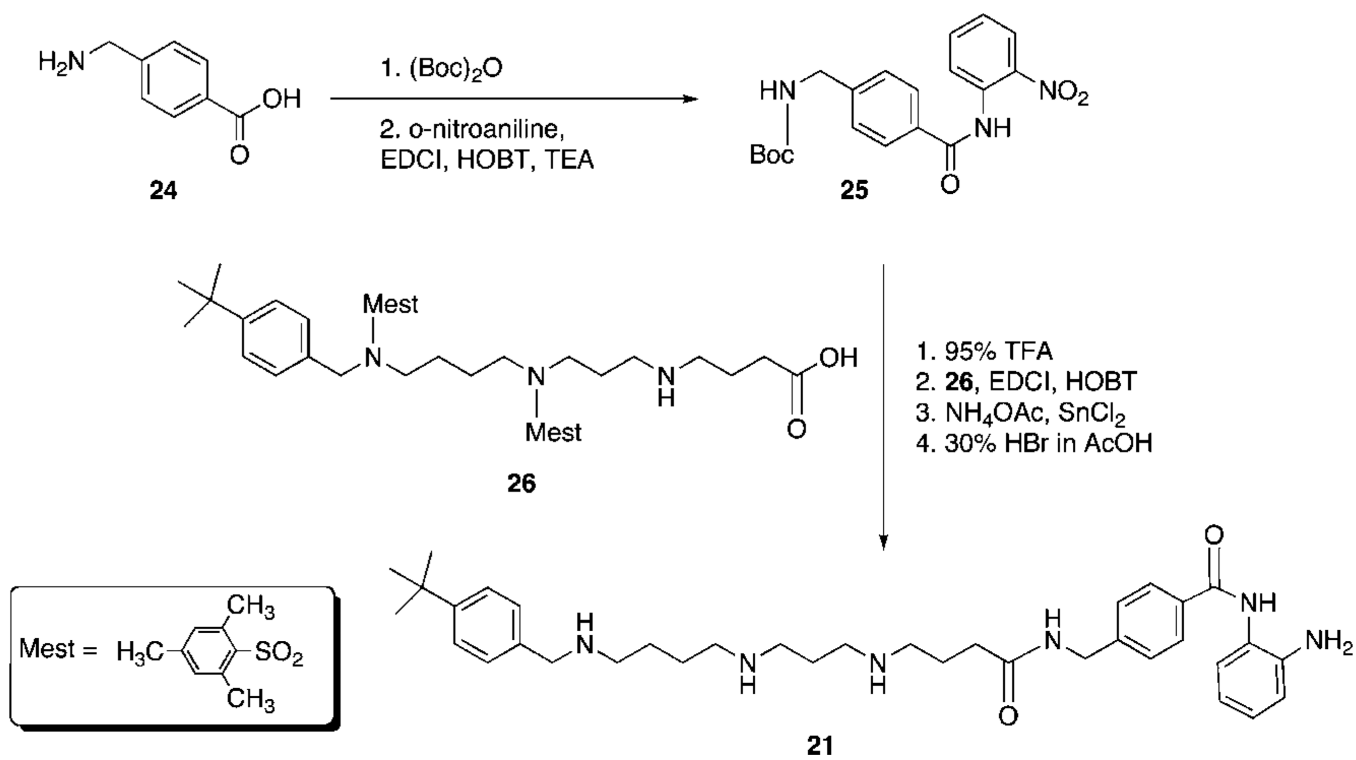


**Figure 4.**

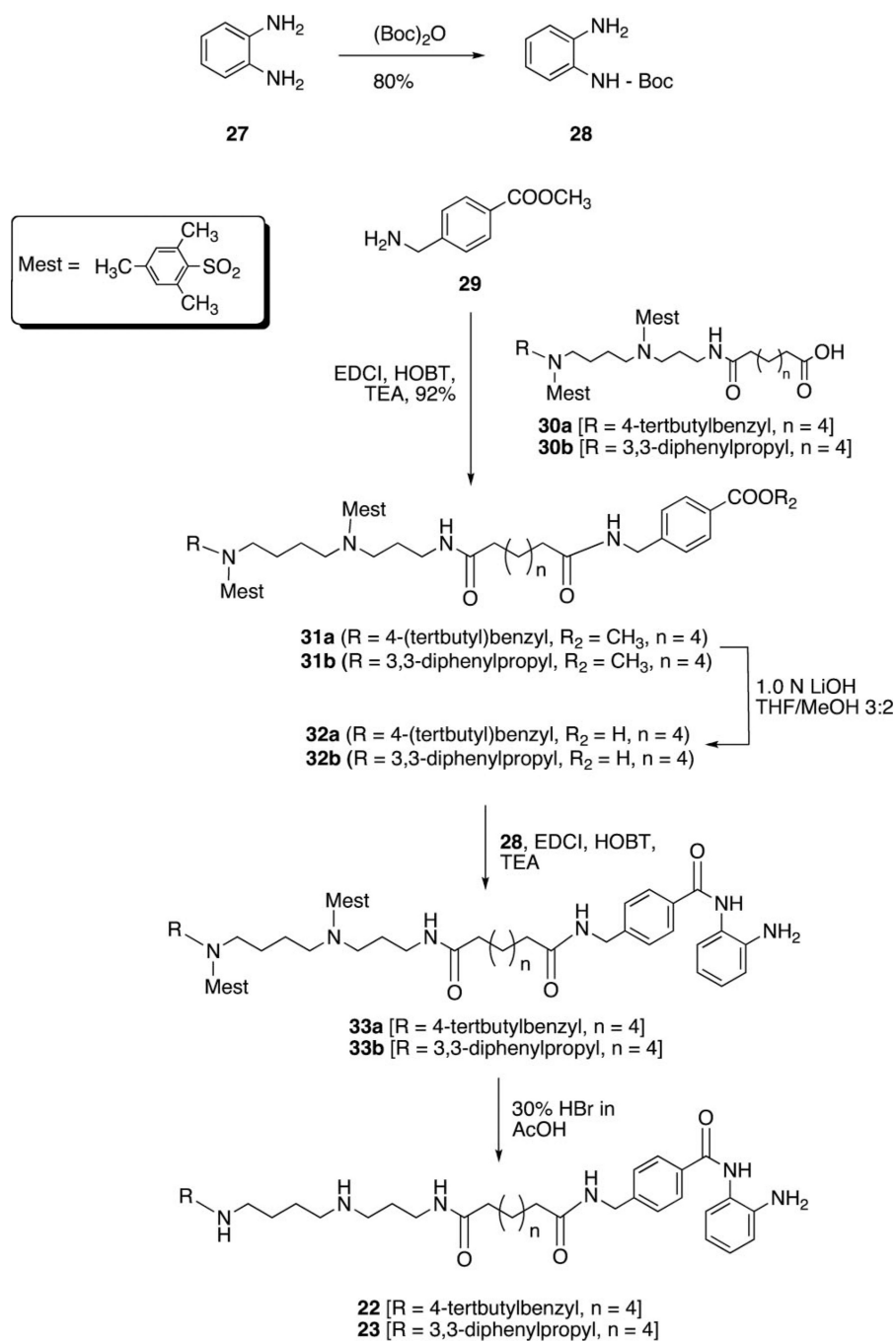
Dose–response data for the re-expression of p16 and p21<sup>waf1</sup> proteins in HCT116 human colon carcinoma cells following 24 h of treatment with PABA **22**, +/- 5-aza-dC pretreatment. Data points are single determinations derived from infrared detection-based quantification of representative Western blots.



**Figure 5.** Inhibition of  $^{14}\text{C}$ -spermidine uptake by compound **21**. The concentration-dependent uptake of  $^{14}\text{C}$ -spermidine was measured over a range of concentrations in the presence of 0.0, 10.0, 25.0, and 50.0  $\mu\text{M}$  concentrations of compound **21**. Each data point is an average of two determinations that differed by <1% in all cases.



Scheme 1.






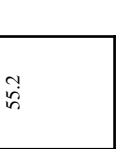
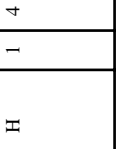
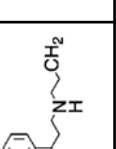
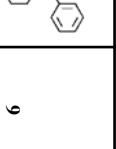
Scheme 2.

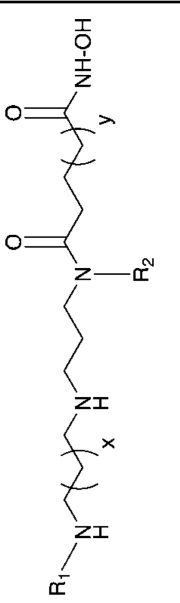
\$watermark-text

\$watermark-text

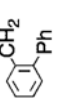
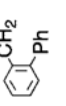
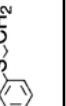
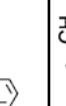
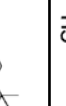
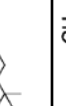
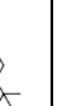

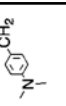
\$watermark-text

**Table 1**Structures of PAHA Analogues **6–20** and Their Inhibitory Activity against HeLa Cell Extract Histone Deacetylase at 1.0  $\mu\text{M}$ 

Compound	R <sub>1</sub>	R <sub>2</sub>	x	y	% inhibition (1.0 $\mu\text{M}$ )
6		H	1	4	55.2
7		H	2	3	46.3
8		H	2	5	54.6
9		H	2	6	73.9
10		H	2	4	46.7
11		H	2	2	15.9
12		H	2	4	41.4



The chemical structure shows a polyamine chain with a terminal secondary amine (R<sub>1</sub>-NH-), a secondary amine with a substituent R<sub>2</sub> (N(R<sub>2</sub>)-), and a terminal primary amine (NH-OH). The chain is composed of two segments: one with x methylene groups and another with y methylene groups. The substituents R<sub>1</sub> and R<sub>2</sub> are defined in the table below.

Compound	R <sub>1</sub>	R <sub>2</sub>	x	y	% inhibition (1.0 μM)
13		H	2	2	71.3
14		H	2	4	38.6
15		H	2	2	6.7
16		H	2	4	16.5
17		H	2	3	51.5
18		H	2	5	88.7
19			2	2	2.0
20	H		2	4	58.6

**Table 2**

Fold Increase in the Re-Expression of p21<sup>Waf1</sup>, Acetylated Histones H3 (AcH3) and H4 (AcH4), and Acetylated  $\alpha$ -tubulin (AcTubulin) Proteins in HCT116 Colon Carcinoma Cells<sup>a</sup>

compd	p21 <sup>waf1</sup>	AcH3	AcH4	AcTubulin
<b>9</b>	0.41	0	0.95	1.97
<b>10</b>	0.46	0	1.36	6.76
<b>11</b>	3.01	3.76	14.22	75.7
<b>12</b>	0.86	0	4.74	11.98
<b>13</b>	2.01	3.34	17.4	89.01
<b>14</b>	1.64	5.19	7.82	36.3
<b>15</b>	2.56	2.38	12.06	72.9
<b>16</b>	1.98	0	11.68	101.36
<b>17</b>	2.33	21.49	20.84	253.25
<b>18</b>	0.61	0	3.25	11.99
<b>20</b>	0.49	0	1.95	6.07
<b>22</b>	2.55	1.19	1.12	2.27
SAHA	1.13	30.65	106.57	13.24

<sup>a</sup>Cells were treated for 24 h with a 10  $\mu$ M concentration of compounds **9–18**, **20**, **22**, and SAHA. Data points are single determinations derived from infrared detection and quantification of representative Western blots.



**Table 3**Cytotoxicity Data for PAHA Analogues **6–20** and PABA Analogues **21–23** in HCT116 Human Colon Cancer Cells<sup>a</sup>

compd	% HDAC inhibition at 1.0 $\mu$ M	IC <sub>50</sub> in wild type HCT 116 cells ( $\mu$ M)
SAHA	100	1.8
<b>6</b>	55.2	>100
<b>7</b>	46.3	>100
<b>8</b>	54.6	>100
<b>9</b>	73.9	>100
<b>10</b>	46.7	>100
<b>11</b>	15.9	>100
<b>12</b>	41.4	>100
<b>13</b>	71.3	>100
<b>14</b>	38.6	>100
<b>15</b>	6.7	>100
<b>16</b>	16.5	>100
<b>17</b>	51.5	>100
<b>18</b>	88.7	>100
<b>19</b>	2.0	ND
<b>20</b>	58.6	38.6
<b>20</b> + 1.0 mM AG	58.6	>100
<b>21</b>	28.0	>100
<b>22</b>	30.8	>100
<b>23</b>	66.7 (5 $\mu$ M)	>100

<sup>a</sup> Cells were treated for 96 h with a range of concentrations of each test compound, and cell viability was measured using a standard MTS reduction assay. Each data point is the average of two separate experiments that differed by <5% in every case, with each data point within an experiment performed in triplicate. AG = aminoguanidine. ND = not determined.